Supplementary Figures/Tables

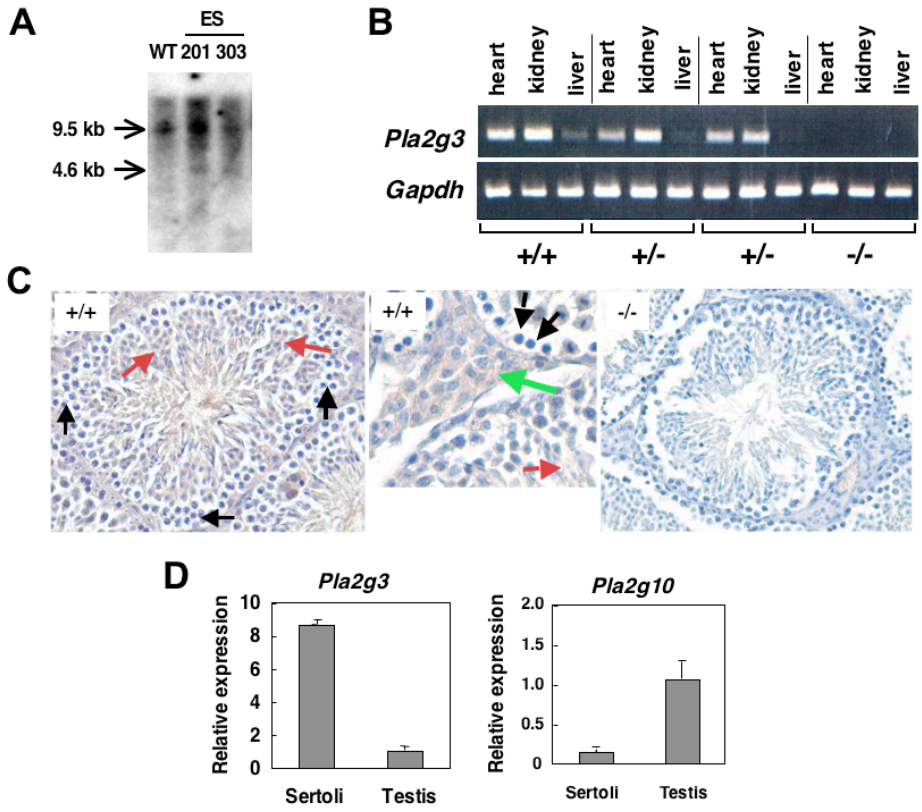

Figure S1

Verification of *Pla2g3* disruption in knockout mice. (A) Genomic DNA from ES cells with WT allele and two ES clones (#201 and #303) with targeted allele after *Sph*I digestion were subjected to Southern blotting. (B) Expression of *Pla2g3* mRNA in various tissues of $Pla2g3^{+/+}$, $Pla2g3^{+/-}$ (2 samples) and $Pla2g3^{-/-}$ mice. *Gapdh* mRNA was used as a control for equal sample loading into each lane. (C) Testis sections from $Pla2g3^{+/+}$ and $Pla2g3^{-/-}$ mice were immunostained with anti-sPLA$_2$-III antibody. In $Pla2g3^{+/+}$ mice, spermatogenic cells (*dark arrows*) were overall negative, whereas Sertoli cells (*red arrows*) and interstitial Leydig cells (*green arrow*) gave positive staining. No staining was found in $Pla2g3^{-/-}$ mice. (D) Real-time PCR analysis of the expression of *Pla2g3* and *Pla2g10* mRNA in cultured mouse Sertoli cells and whole testis, with the expression in the testis being regarded as 1. Data are normalized with the expression of 18S ribosomal RNA. Values are mean $\pm$ S.D. (n = 4).

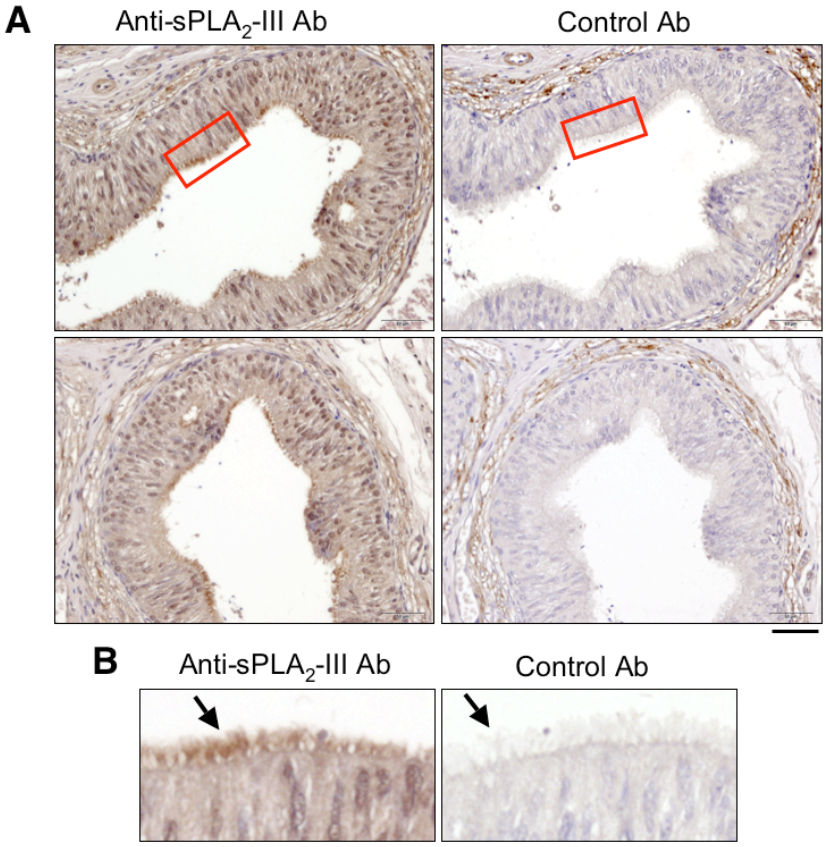

Figure S2

Immunohistochemistry of sPLA$_2$-III in human epididymis.

Human epididymal sections were stained with anti-sPLA$_2$-III (*left*) and control (*right*) antibodies. Two representative photos for each are shown. The epithelial layer showed intense staining of sPLA$_2$-III (A). When boxed areas in (A) were magnified, staining of luminal cilia (*arrows*) by anti-sPLA$_2$-III antibody was evident (B), suggesting that sPLA$_2$-III is secreted into the lumen. Staining of the interstitium beneath the epithelium was non-specific, since it was equally stained by anti-sPLA$_2$-III and control antibodies (A). A scale bar represents 60 μm.

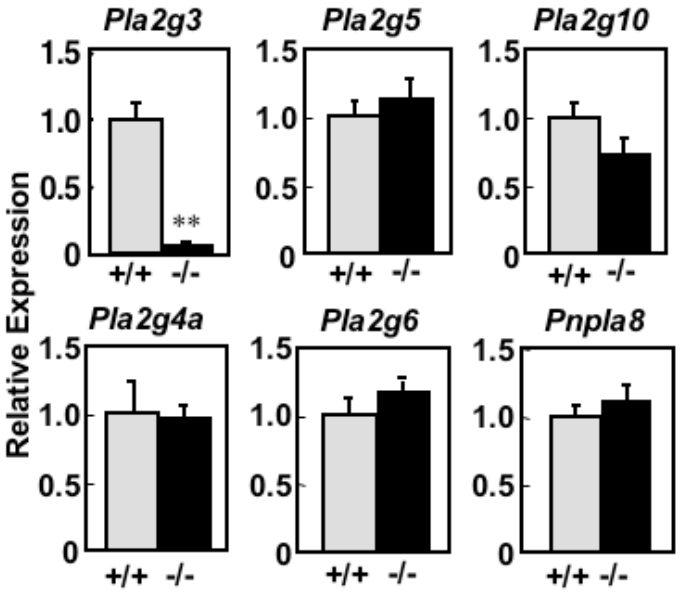

Figure S3

Expression of various PLA_2s in *Pla2g3*-deficient epididymis. The epididymal expression levels of six PLA_2 enzymes in *Pla2g3*$^{+/+}$ (*grey bars*) and *Pla2g3*$^{-/-}$ (*solid bars*) mice were assessed by quantitative RT-PCR (mean $\pm$ S.D. (n = 5)).

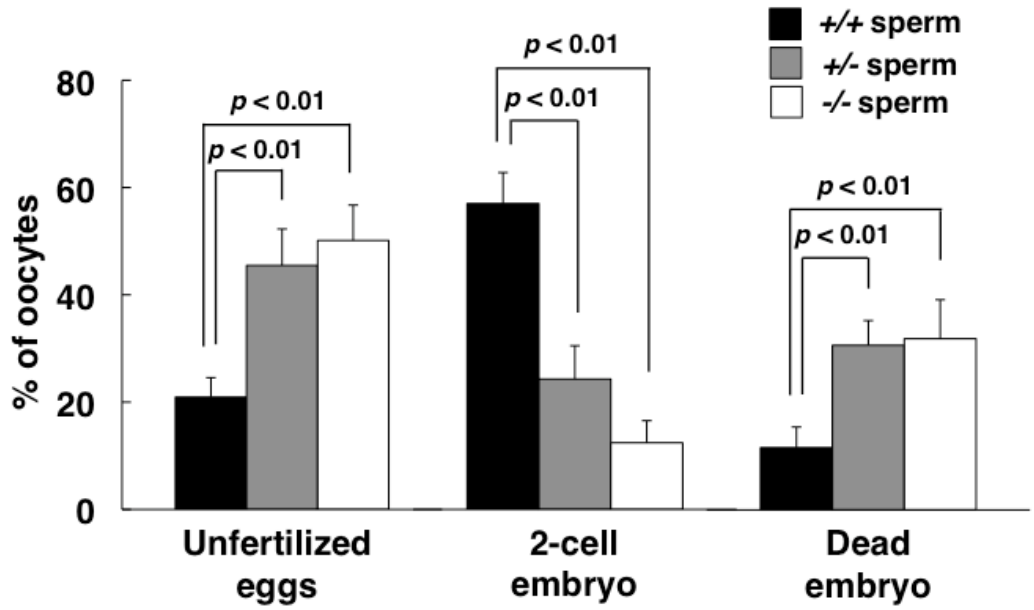

Figure S4

Impaired IVF of *Pla2g3*-deficient spermatozoa. IVF was performed by mixing wild-type oocytes with *Pla2g3*$^{+/+}$ (n = 14), *Pla2g3*$^{+/-}$ (n = 15) or *Pla2g3*$^{-/-}$ (n = 12) spermatozoa. After 24 h, unfertilized eggs, 2-cell embryos and dead embryos were counted. In accordance with the reduction of 2-cell embryos (an indication of successful fertilization), both unfertilized eggs and dead embryos were increased by *Pla2g3* deficiency in a gene dosage-dependent manner.

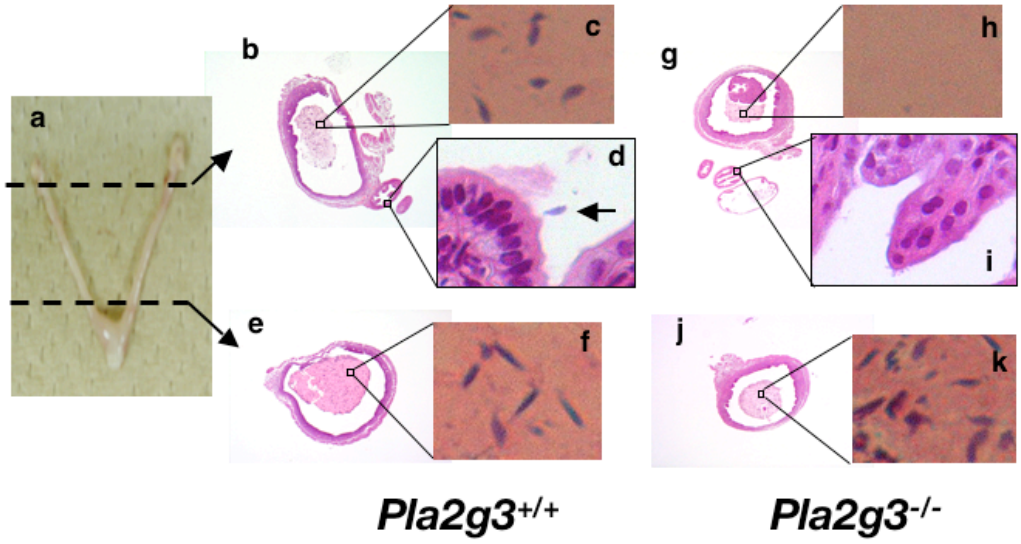

Figure S5

Impaired transit of *Pla2g3*$^{-/-}$ sperm through the female genital tract after coitus. Sixteen hours after mating of *Pla2g3*$^{+/+}$ (*panels a and b*) and *Pla2g3*$^{-/-}$ (*panels c and d*) male mice with female C57BL/6 mice, the uterine ducts were isolated from the females, and paraffin-embedded sections of the utero-tubal junction and lower part of the uterus *(panel a*, dashed lines) were stained with hematoxylin and eosin. Gross views of the cross-sections indicated the presence of seminal plasma in the uterine ducts in both *Pla2g3*$^{+/+}$ (*panels b and e*) and *Pla2g3*$^{-/-}$ (*panels g and j*) mice. Boxed areas are magnified in *panels c, d, f, h, i* and *k*. Spermatozoa of *Pla2g3*$^{+/+}$ mice were distributed in all areas of the uterine duct (*panels c and f*) and even in the oviduct (*panel d*; indicated by the arrow), whereas those of *Pla2g3*$^{-/-}$ mice remained in the lower uterus (*panel k*) and were barely found in the upper uterus (*panel h*) and oviduct (*panel i*).

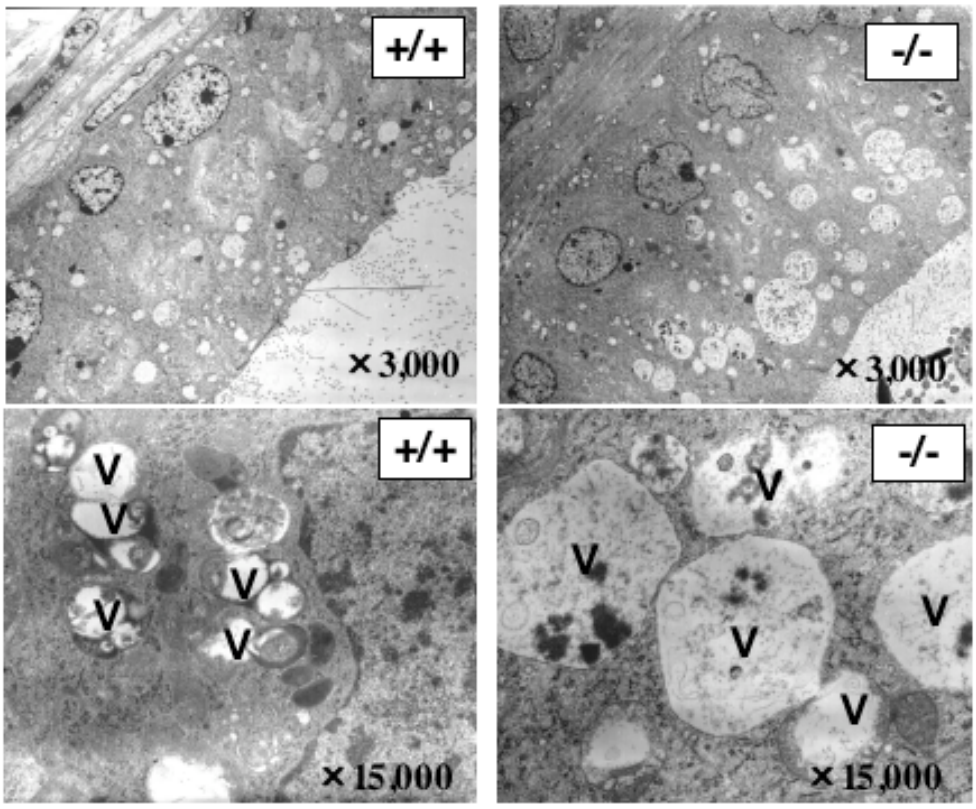

Figure S6

Ultrastructure of the caput epididymal epithelium as assessed by transmission electron microscopy. Cytoplasmic vesicles (V) in the caput epididymal epithelium of *Pla2g3*$^{-/-}$ mice were larger than those of *Pla2g3*$^{+/+}$ mice.

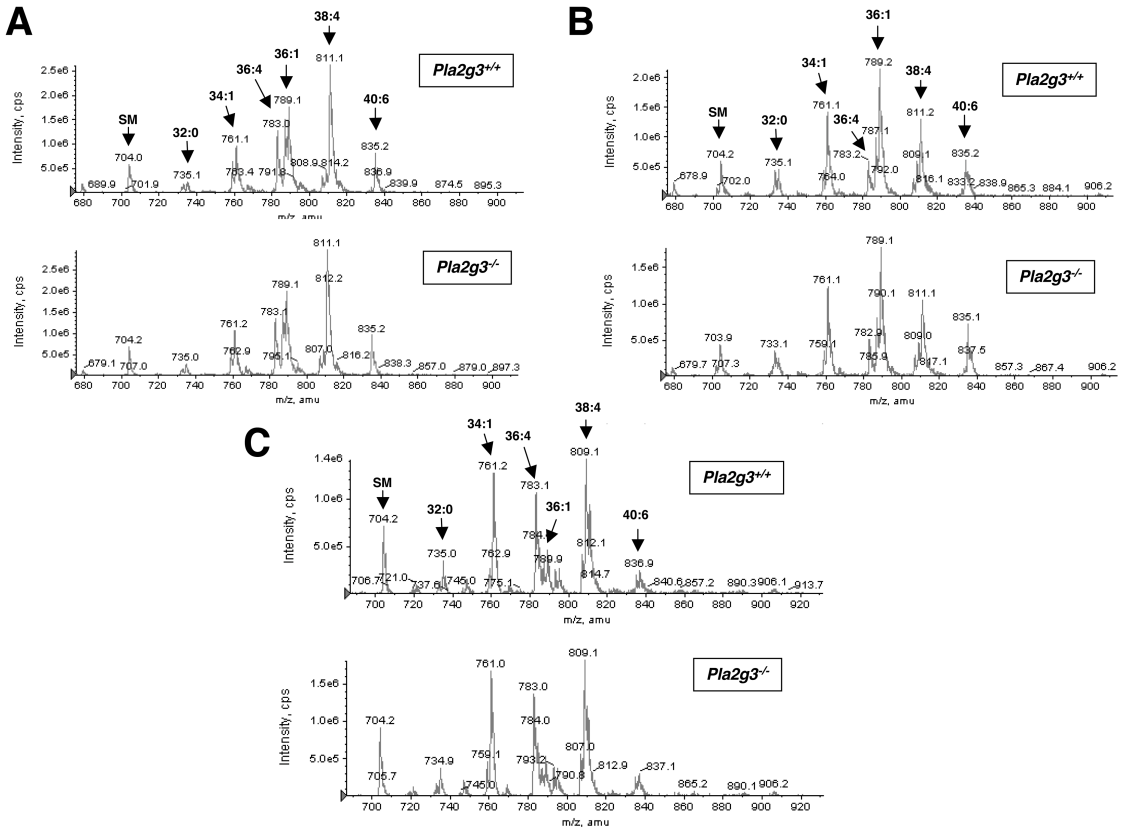

Figure S7

ESI-MS analysis of PC molecular species in male gonads. ESI-MS spectra of PC in the sperm-depleted caput (A) and cauda (B) epididymis and in the testis (C) of *Pla2g3*$^{+/+}$ (*upper panel*) and *Pla2g3*$^{-/-}$ (*lower panel*) mice. Representative results of three independent experiments are shown. Major peaks of PC molecular species are indicated by arrows. There were no significant differences in PC fatty acid composition between the genotypes. SM, sphingomyelin.

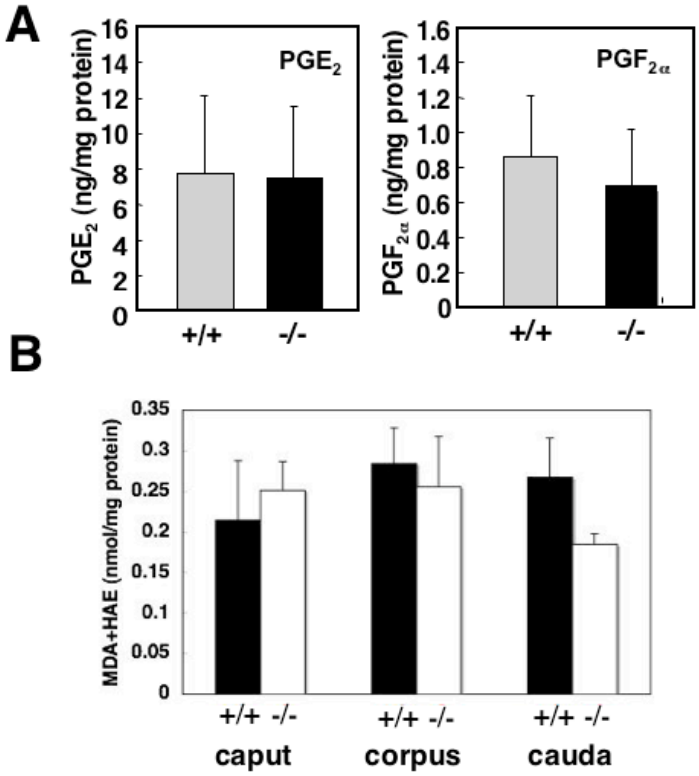

Figure S8

Evaluation of the levels of gonadal prostaglandins and lipid peroxidation. (A) PGE_2 (*left panel*) and $PGF_{2\alpha}$ (*right panel*) in epididymal fluid of *Pla2g3*$^{+/+}$ (*grey columns*) and *Pla2g3*$^{-/-}$ (*solid columns*) mice were quantified using enzyme immunoassay kits (mean $\pm$ S.D. (n = 5)). (B) Levels of lipid peroxidation in distinct portions of the epididymis from *Pla2g3*$^{+/+}$ (*solid columns*) and *Pla2g3*$^{-/-}$ (*clear columns*) mice were quantified using an LPO assay kit (mean $\pm$ S.D. (n = 5)).

Table S1

Counts of cauda epididymal sperm, weights of testis, epididymis and body, and concentrations of serum testosterone in *Pla2g3*$^{+/+}$, *Pla2g3*$^{+/-}$ and *Pla2g3*$^{-/-}$ male mice.

Values are mean ± S.D. (n = 5~7).

Genotypes	Sperm count x10^7	Testis weight g	Epididymis weight g	Body weight g	Serum testosterone ng/ml
+/+	2.20 ± 0.38	0.21 ± 0.08	0.084 ± 0.007	28.2 ± 0.92	0.179 ± 0.047
+/-	2.50 ± 0.33	0.21 ± 0.01	0.073 ± 0.003	32.4 ± 2.21	0.190 ± 0.055
-/-	1.90 ± 0.74	0.22 ± 0.01	0.075 ± 0.003	28.7 ± 1.00	0.181 ± 0.086